Moriguchi, Kai; Ueki, Tatsuhito; Saito, Masashi

**Article**

# Establishing optimal forest harvesting regulation with continuous approximation

Operations Research Perspectives

**Provided in Cooperation with:**
Elsevier

*Suggested Citation:* Moriguchi, Kai; Ueki, Tatsuhito; Saito, Masashi (2020) : Establishing optimal forest harvesting regulation with continuous approximation, Operations Research Perspectives, ISSN 2214-7160, Elsevier, Amsterdam, Vol. 7, pp. 1-13, https://doi.org/10.1016/j.orp.2020.100158

Operations Research Perspectives 7 (2020) 100158

Contents lists available at ScienceDirect

Operations Research Perspectives

journal homepage: www.elsevier.com/locate/orp

# Establishing optimal forest harvesting regulation with continuous approximation

Kai Moriguchi[a,*], Tatsuhito Ueki[b], Masashi Saito[c]

[a] Faculty of Agriculture and Marine Science, Kochi University, 200 Otsu, Monobe, Nankoku, Kochi 783-8502, Japan
[b] Faculty of Agriculture, Shinshu University, 8304 Minami-Minowa, Kami-Ina, Nagano 399-4598, Japan
[c] Faculty of Agriculture, Iwate University, 3-18-8 Ueda, Morioka, Iwate 020-8550, Japan

ARTICLE INFO

*Keywords:*
Forest harvesting regulation
Continuous approximation
Net present value
Simulated annealing

ABSTRACT

While optimal forest harvesting regulations (regional forest regeneration schedules) have been established using the linear programming technique, its modeling restriction is still a challenge in practice. In this study, we developed an alternative framework for establishing an optimal forest harvesting regulation using the continuous approximation technique. The regulation problem was reformulated as a problem to find optimal smooth control of regeneration area, thereby overcoming the difficulties in finding the global optimum for the optimization models that include nonlinear or more complex models. A seven-dimensional optimization model was developed involving efficient assurance of the convergence to a stable forest state and prohibition of clearcutting in immature stands. Using this model, we established optimal forest harvesting regulations in Nagano Prefecture, Japan. Simulated annealing was utilized to explore optimal solutions. Analyses based on extreme value theory and comparison with solutions produced by grid search indicated that the best solutions may be sufficiently close to global optima. The best solutions suggested controlling timber supply to keep prices high in the early years, due to the supply–demand log price model and the use of net present value as the objective function. Because of the low profitability of the region, the solution suggested delaying the achievement of the target state as far as possible.

## 1. Introduction

Forestry has a much longer crop rotation cycle compared to other agricultural systems. Optimal rotation age, the forest age at which clearcutting provides maximum net profit, can often be more than half a century [1–3]. The long rotation cycle implies that forest owners who planted their forests may not always benefit from the crop while they are alive. Therefore, without any regulation, it is possible that forest owners neglect reforestation after clearcutting, which results in deforestation. Another problem is overcutting in immature stands. This may occur when there is a shortage of timber supply compared with timber demand. If rotation ages are too short, forest lands are overused, and forest degradation occurs. These problems can result in the decline of available forest stock, increases in greenhouse gas emissions [4], and degradation of biodiversity [5]. As a result, and at the very least, wide-scale generational cooperation among forest owners may be needed to prevent such problems. However, without a guide, controlling regional forests with multiple owners is not a simple mission. Consequently, a regional forest regeneration (clearcutting and the following reforestation) schedule with enforcement of reforestation and prohibition of clearcutting in immature stands, so-called forest harvesting regulation (FHR), may be needed even in regions where most forest stands are privately owned.

We should also note that FHR constrains forest owners with respect to their choice of rotation age. In other words, an FHR may force the forest owners to choose a suboptimal rotation age. Therefore, an FHR should be, at least, established optimally for accountability for the forest owners. Optimal forest harvesting schedules have been established by several researchers, depending on the characteristics of the regions and the objectives of forest use [6]. One approach is to identify an optimal harvesting schedule for each forest stand in the subject region [7–11]. This approach can provide concrete schedules as to which forest stands should be regenerated during each period, taking the spatial constraints between each forest stand into account. On the other hand, when applying the approach in forest areas with numerous private owners, the concrete schedule might be an obstacle in practice because it does not allow any change by the forest owners with respect to rotation age. As a result, although this type of schedule is effective for forests owned by a single owner or a few owners, the schedule might be too strict as a regional schedule of forest regeneration. Therefore, in

*Abbreviations:* FHR, forest harvesting regulation; NPV, net present value; DNF, destination normal forest

* Corresponding author.
*E-mail addresses:* k_moriguchi@kochi-u.ac.jp (K. Moriguchi), tatueki@shinshu-u.ac.jp (T. Ueki), msaito@iwate-u.ac.jp (M. Saito).

https://doi.org/10.1016/j.orp.2020.100158
Received 30 December 2019; Received in revised form 14 April 2020; Accepted 22 June 2020
Available online 26 June 2020

practical cases, the FHR in a region is often established in laxer form: by identifying optimal control of the forest area for each forest type in the region, rather than considering spatial properties of each stand. Hereafter we use “FHR” for indicating this type of schedule.

The FHRs have usually been established using the linear programming (LP) technique [12–15]. Treating the area of each age-class (classified stand ages, such as 1- to 5-year-old stands into class 1, 6- to 10-year-old stands into class 2, and older stands as well) of each period in the FHR as the decision variables, and formulating the FHR as the control problem of the age-class distribution (forest area distribution on the age-class) over time, an FHR can be formulated as an LP problem. The advantage of using the LP technique is that the identification of a global optimum in polynomial time is assured [16–18]. By contrast, we have a great constraint in modeling: we cannot use nonlinear models in most cases,[1] whereas models related to forest management are often nonlinear. As a result, although the LP technique for the FHR has been developed, the scope of the optimization model is still limited so that nonlinear phenomena that violate the linearity in the optimization model are not incorporated.

Recently, a few researchers used nonlinear programming (NLP) to find optimal forest management strategies [19]. However, we should note that there is no assurance that a global optimum can be identified for general nonlinear models. If we only create the nonlinear optimization model for the FHR by simply extending the ordinary formulation that is originally assumed to be solved with the LP technique, the model will have numerous variables and large search space. As a result, it is possible that we may obtain local optima rather than a global optimum [19,20]. The use of the approximation method of nonlinear programming models using mixed-integer linear programming models is a means of overcoming the difficulty in finding the global optimum [21]. However, the increase of the number of integer variables associated with the linear approximation may cause considerable increase of computation time; this also causes a difficulty in finding the global optimum in practice. These difficulties seem to be the fundamental reason that FHRs have rarely been modeled as NLP problems.

A possible way to develop an FHR with nonlinear models is to develop an optimization model so that it can be optimized with existing techniques. This is similar to the way we have modeled the FHR problem so that it can be solved with the LP technique. For example, if we can construct the model so that the objective function is convex, the model can be optimized with a simple downhill method such as Newton's method. Another possible way is to devise optimization algorithms using the features of objective optimization models [22]. However, we should note that the models and principles in regional forest management vary greatly owing to both the diversity among regions and the diverse management principles and concerns of each planner. Moreover, on a regional scale, it seems necessary to consider the price changes due to the balance of supply and demand. The models tend to be complex and diverse due to strategic interactions between suppliers and consumers [23–25]. As a result, developing specific models that can be optimized with specific optimization techniques or model-specific optimization techniques may cause problems similar to the FHR problems that arise from the use of LP.

On the other hand, the dynamics of age-class distribution with time and the optimality have been analyzed theoretically and computationally [26–31]. It indicates that the FHR problem is fundamentally the optimization of the control of the dynamics of age-class distribution. In other words, the FHR can be established with the optimization of parameters of system dynamics simulation [32–35]. In practice, the control of the annual total regeneration area in a region should be smooth. For example, even if the optimal solution suggests that the annual total regeneration area should be 5 ha, 50 ha, and 5 ha for three consecutive years, the solution may not be practical. Similar smoothness is required in the regeneration area between different stand ages at a time. For example, even if an optimal FHR suggested 90% regeneration (in forest area) for 40- and 42-year-old stands but 10% regeneration for 41-year-old stands, the solution may not be practical.

These requirements indicate that the FHR problem can be modeled as an optimization problem with the few parameters of the smooth control. The conversion can be done using the continuous approximation technique [36–38], which translates a discrete model to a continuous model, thereby reducing the dimensionality of the optimization problem. The reduction of dimensionality enables us to introduce diverse models into the FHR models since the reduction enhances the ability to identify exact solutions. The reformulation itself is not complex for the FHR problem; however, for the efficient generation of feasible solutions, the constraints in FHR models should be re-developed.

In this study, we developed an optimization model to establish optimal FHR using the continuous approximation technique. The constraints for the control of age-class distributions that involves the prevention of clearcutting immature stands and achievement of a stable state in the age-class distribution at the end of a planning horizon were developed. We then applied this approach for the establishment of FHRs for Nagano Prefecture, Japan. The remainder of this paper is structured as follows. In Section 2, we develop the objective model. In Section 3, the application for the establishment of FHRs for the Nagano Prefecture is presented. Finally, the applicability of the continuous approximation technique for the FHR in other situations is discussed.

## 2. Model development

The FHR is established as optimal control of the age-class distribution of a set of forests, thereby gaining maximum utility (or minimum loss) from forests at present value. Let us denote the stand age, the year since regeneration, as $\tau$ (year; positive integers starting with 1). Generally, an age-class can be defined with multiple ages, such as 1- to 5-year-old stands into class 1, 6- to 10-year-old stands into class 2, and older stands as well [19,39]. In the ordinary LP formulation, the class grouping reduces the dimensionality of the problem. In contrast, for simplicity, we define each age-class as corresponding directly with the stand age. Therefore, age-class-1 indicates 1-year-old stand age, age-class-2 indicates 2-year-old stand age, and so on. Similarly, in this study, the time period from the start of the schedule denoted as $t$ (positive integers starting with 1) is equivalent to the year from the start. $t = 1$ is the first year of the schedule, $t = 2$ is the second year of the schedule, and so on. We use stand age to identify an age-class, and year to identify a time period for simplicity. If humans regenerate a $\tau$-year-old stand at $t$, the age of the stand will be one at the next year ($t + 1$). The stand area of 1-year-old stands at $t + 1$ is thus the total of the regenerated area at $t$. If a stand is not regenerated, the age of the stand will be $\tau + 1$ at the next year.

FHRs are often required to achieve a stable and sustainable age-class distribution (such as the state of “normal forest,” introduced later) at the end of a schedule [40]. FHRs can also be established without this constraint. However, because the FHR model involves the discrete-time control of the dynamics of age-class distribution, the destination states of an optimal FHR can include a cyclic fluctuation in age-class distribution [29,30,41] similar to the behavior of a discrete-time logistic map [42]. It has been established that stable age-class distribution can be the convergence state of the optimal FHR with the continuous-time models [26].

Because such cyclic fluctuations of age-class distributions may be problematic from a practical standpoint, some desire the FHR to achieve a given stable age-class distribution, called the normal forest [43], which has a rectangular-shaped age-class distribution owing to constant stand area per stand age and identical rotation age, at the end

[1] Simple and specific nonlinear models such as geometric decline of the present value factor and simplified forest growth model do not violate the linearity of the optimization problem and can be used in the LP formulation (described in Section 2.2).

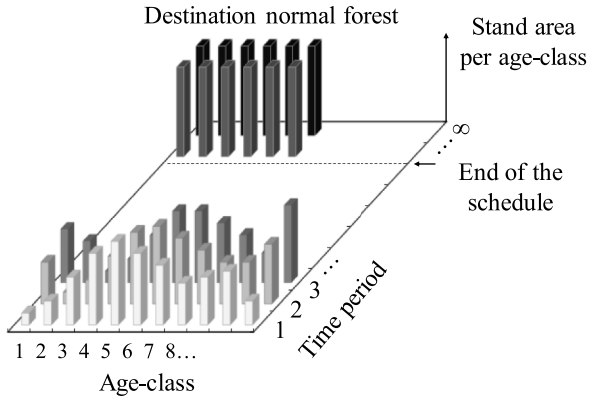


**Fig. 1.** Concept of forest harvesting regulation (FHR). Each horizontal bar set (with identical color) indicates the age-class distribution at each time period. Starting at a given age-class distribution, we manage the age-class distribution optimally, aiming for a destination normal forest (DNF) at the end of the schedule.

of the schedule. We denote the normal forest to be achieved as destination normal forest (DNF). We also assume that when the DNF is achieved, all conditions of forest management, such as log price, will be stable, and consequently, the annual revenue will be constant. Although both realizing a normal forest and the assumption of a steady-state are unrealistic 'ideals,' it enables us to consider forest utility in infinite terms, whereas FHR models without those assumptions consider the net present value (NPV) with a finite time horizon. The concept of the FHR is shown in Fig. 1. Letting $t_F$ be the year until we achieve the DNF (year; virtual time horizon) and $\tau_U$ the possible maximal stand age (year), the optimal FHR problem can be formulated as an optimal control problem of stand area for all $t$ in $\{1, 2, \ldots, t_F\}$ and all $\tau$ in $\{1, 2, \ldots, \tau_U\}$.

Since the whole model is large, we formulate the model in four separate sections below.

### 2.1. Objective function and basic models

The objective function and basic models are formulated as follows (without notations, all constraints imply $\forall t \mid t \in \{1, 2, \ldots, t_F\}$, or $\forall \tau \mid \tau \in \{1, 2, \ldots, \tau_U\}$, or both):

$$\max \text{NPV} = \sum_{t=1}^{\infty} D_t U_t = \sum_{t=1}^{t_F} D_t U_t + \frac{100}{d} D_{t_F} U_{NF} \tag{1}$$

s.t.

$$D_t = \frac{1}{(1 + d/100)^t} \tag{2}$$

$$U_t = \sum_{\tau=\tau_{Lt}}^{\tau_U} u_{t,\tau} \tag{3}$$

$$u_{t,\tau} = [y_\tau (p_t - c_C) - c_R] r_{t,\tau} \tag{4}$$

$$a_{t+1,\tau+1} = a_{t,\tau} - r_{t,\tau} \tag{5}$$

$$a_{t+1,1} = R_t \tag{6}$$

$$0 \le r_{t,\tau} \le a_{t,\tau} \tag{7}$$

$$R_t = \sum_{\tau=\tau_{Lt}}^{\tau_U} r_{t,\tau} \tag{8}$$

$$r_{t,\tau}=0 \quad \forall\ \tau \mid \tau<\tau_{Lt} \tag{9}$$

$$a_{t_F+1,\tau} = a_{NF,\tau} = \begin{cases} R_{NF} \forall\ \tau \mid \tau \le \tau_{NF} \\ 0 \ \forall\ \tau \mid \tau > \tau_{NF} \end{cases} \tag{10}$$

$$\sum_{\tau=1}^{\tau_U} a_{t,\tau} = R_{NF}\, \tau_{NF} \tag{11}$$

where NPV is the net present value in yen, $D_t$ is the present value factor at $t$, $U_t$ is the annual revenue at $t$ from the set of forests (yen), $U_{NF}$ is the annual revenue from the set of forests after achieving the DNF (yen), $d$ is the annual interest rate (%), $\tau_{Lt}$ is the lower bound of the regenerable stand age at $t$ (year), $u_{t,\tau}$ is annual revenue at $t$ from $\tau$-year-old stands (yen), $y_\tau$ is the mean yield per area of $\tau$-year-old stands ($m^3$/ha), $p_t$ is the log price at $t$ (yen/$m^3$), $c_C$ is a constant clearcutting cost (yen/$m^3$), $r_{t,\tau}$ is annual regeneration area of $\tau$-year-old stands at $t$ (ha), $c_R$ is a constant reforestation cost (yen/ha), $a_{t,\tau}$ is the area of $\tau$-year-old forests at $t$ (ha), $R_t$ is the annual total regeneration area at $t$ (ha), $a_{NF,\tau}$ is the area of $\tau$-year-old forests of the DNF (ha), $R_{NF}$ is the annual total regeneration area after achieving the DNF (ha), and $\tau_{NF}$ is the rotation age of the DNF (year). All variables except for $t$, $\tau$ and their specific values ($\tau_{Lt}$, $\tau_U$, $\tau_{NF}$, and $t_F$) are real numbers. All other variables appearing in the remainder of the paper are real numbers.

The right side of Eq. (1) is derived using the formula of geometric series, based on the assumption that the annual revenue is constant after achieving the DNF. Eq. (2) has $d$ and $t$, both are given values, in the argument. Therefore, the value of $D_t$ at each $t$ is constant. Eqs. (3) and (4) indicate that $U_t$ is calculated with a simple balance equation of profits and costs. In Eq. (3), $\tau_{Lt}$ is mainly defined considering the capacity of forest use discussed in Section 2.4. By contrast, $\tau_U$ is defined considering computing capacity to treat all the possible stand ages; we can set the value by adding $t_F$ to the maximum stand age of the present. Eqs. (5)–(8) express the dynamics of the age-class distribution. Eq. (9) expresses the prohibition of regeneration in immature stands. Eq. (10) indicates that the DNF must be obtained after regeneration at $t_F$. Eq. (11) indicates the total area of forests must be identical to that of the DNF throughout the schedule.

The decision variables that can be controlled by forest managers are $r_{t,\tau}$. Furthermore, Eq. (10) indicates $r_{t_F+1,\tau_{NF}} = a_{NF,\tau_{NF}}$ and $r_{t_F+1,\tau} = 0\ \forall \tau \mid \tau \neq \tau_{NF}$. Therefore, the search space of the problem is $\mathbf{R}^{t_F \times \tau_U}$.

### 2.2. Nonlinear models

We used the yield model defined as Eq. (12) and log price model defined as Eqs. (13)–(15):

$$y_\tau = y_\infty [1 - L_y \exp(-k_y \tau)]^{m_y} \tag{12}$$

$$p_t = \max\left\{p_L, \min\left\{\left(\frac{Y_t}{Y_t'} - 1\right)k_p + p_S, p_U\right\}\right\} \tag{13}$$

$$Y_t = \sum_{\tau=\tau_{Lt}}^{\tau_U} y_\tau r_{t,\tau} \tag{14}$$

$$Y_t' = (Y_{NF}' - Y_0') \cdot \varsigma'(t;\ k_{Y'},\ g_{Y'},\ 0,\ t_{Y'U}) + Y_0' \tag{15}$$

$$\varsigma'(x;\ k,\ g,\ x_L,\ x_U) = \begin{cases} 0 & \text{if } x < x_L \\ \frac{\varsigma(x;\ k,g) - \varsigma(x_L;\ k,g)}{\varsigma(x_U;\ k,g) - \varsigma(x_L;\ k,g)} & \text{if } x_L \le x \le x_U \\ 1 & \text{if } x > x_U \end{cases} \tag{16}$$

$$\varsigma(x;\ k,\ g) = \frac{1}{1 + \exp[-k(x - g)]} \tag{17}$$

where $y_\infty$, $L_y$, $k_y$ and $m_y$ are given parameters of the growth model, $p_L$ and $p_U$ are the lower and upper bounds of log price (yen/$m^3$), respectively, $p_S$ is the standard log price (yen/$m^3$), $k_p$ ($<0$) is the slope parameter of the log price model, $Y_t$ is the annual total yield from the set of forests at $t$ ($m^3$/year), $Y_t'$ is the annual yield at $t$ to make the log price be $p_S$ ($m^3$/year), $Y'_{NF}$ and $Y'_0$ are annual yields of the DNF and at the start of the schedule ($m^3$/year), respectively, $k_{Y'}$, $g_{Y'}$ and $t_{Y'U}$ are given parameters, $\varsigma(x; k, g)$ denotes the logistic function ($0 < \varsigma(\cdot) < 1$)

with steepness $k$ and inflection point $g$ (when $k > 0$ then $d\varsigma/dt > 0$, $k = 0$ then $d\varsigma/dt = 0$ and $d\varsigma/dt < 0$ otherwise), and $\varsigma'(x; k, g, x_L, x_U)$ is the logistic function which is scaled so that the values at $x$ in $[x_L, x_U]$ are in [0, 1].

Eq. (12) presents the forest stock of each stand age modeled with Bertalanffy–Richards model [44,45]. See Appendix A for the derivation. Eq. (13) is the price model considering discrepancy from "standard" wood supply at $t$ (a supply which makes the log price be $p_S$) with the lower and upper bounds of prices. Because $k_p < 0$, the model indicates the log price at a given $t$ decreases with the increase of annual total yield. See Appendix B for the modeling.

Since the right side of Eqs. (12) and (15) have only given parameters and only either $\tau$ or $t$ in their arguments, $y_\tau$ and $Y'_t$ at each $\tau$ or $t$ is constant. As a result, the linearlity could be kept even with these models. By contrast, Eq. (13) violates the linearity of the optimization problem since $Y_t$, provided with $r_{t,\tau}$, is needed for the calculation.

### 2.3. Smooth control of regeneration area

The changes in annual total regeneration area and difference of regeneration rates between stand ages should be smooth. We model the constraints for the smoothness using the logistic function. Because the control of the annual total regeneration area is critical to achieving DNF, we used a procedure that determines the annual total regeneration area of each year first, then allocates the regeneration area into each stand age of each year. The following are the constraints for the controls:

$$R_t = \min\left\{(R_{NF} - R_0)\cdot \varsigma'(t; k_R, g_R, 0, t_F - \tau_{NF}) + R_0,\ \sum_{\tau=\tau_{Lt}}^{\tau_U} a_{t,\tau}\right\} \tag{18}$$

$$r_{t,\tau} = \psi_{t,\tau} a_{t,\tau} \tag{19}$$

$$0 \le \psi_{t,\tau} \le 1 \tag{20}$$

$$R'_t = \sum_{\tau=\tau_{Lt}}^{\tau_U} \phi_{t,\tau} a_{t,\tau} \tag{21}$$

$$\phi_{t,\tau} = \varsigma\left[\tau; (\alpha_{\phi k} - \beta_{\phi k})\frac{t}{t_F} + \beta_{\phi k}, (\alpha_{\phi g} - \beta_{\phi g})\frac{t}{t_F} + \beta_{\phi g}\right] \tag{22}$$

$$\psi_{t,\tau} = \begin{cases} \xi_t \phi_{t,\tau} & \text{if } R_t < R'_t \\ \phi_{t,\tau} & \text{if } R_t = R'_t \\ (1 - \xi_t) + \xi_t \phi_{t,\tau} & \text{if } R_t > R'_t \end{cases} \tag{23}$$

$$\xi_t = \begin{cases} \frac{R_t}{R'_t} & \text{if } R_t < R'_t \\ \frac{R_t - \sum_{\tau=\tau_{Lt}}^{\tau_U} a_{t,\tau}}{R'_t - \sum_{\tau=\tau_{Lt}}^{\tau_U} a_{t,\tau}} & \text{if } R_t > R'_t \end{cases} \tag{24}$$

where $R_{NF}$ and $R_0$ are the annual total regeneration areas of the DNF and at the start of the schedule (ha), respectively, $k_R$ and $g_R$ are controllable parameters, $\psi_{t,\tau}$ is the regeneration rate of $\tau$-year-old stands at $t$, $\phi_{t,\tau}$ is the variable to control the regeneration rate of $\tau$-year-old stands at $t$, which we call regeneration intensity in this paper, $\alpha_{\phi k}$, $\beta_{\phi k}$, $\alpha_{\phi g}$, and $\beta_{\phi g}$ are controllable parameters that allow the changes-with-time of both the steepness and inflection point of the logistic function, and $\xi_t$ is a utility variable to assure Eq. (8) for a given $R_t$ with the control of Eqs. (19)–(24). Since the annual total regeneration area cannot be larger than the total area of regenerable stands, $R_t$ should be given as Eq. (18).

If $R_t = R'_t$, $\phi_{t,\tau}$ is acceptable as the value of $\psi_{t,\tau}$. For the case of $R_t < R'_t$, Eqs. (19) and (21)–(24) can prepare the annual regeneration area of each stand age so that Eq. (8) is satisfied as follows:

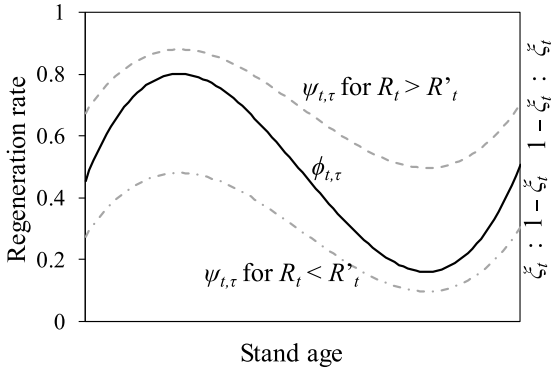


**Fig. 2.** Preparation of the regeneration rate. In the case of $R_t < R'_t$, $\psi_{t,\tau}$ is prepared by decreasing $\phi_{t,\tau}$ as the dashed and dotted line. In the case of $R_t > R'_t$, $\psi_{t,\tau}$ is prepared by increasing $\phi_{t,\tau}$ while keeping $\psi_{t,\tau} < 1$ as the dashed line.

$$\sum_{\tau=\tau_{Lt}}^{\tau_U} r_{t,\tau} = \sum_{\tau=\tau_{Lt}}^{\tau_U} \psi_{t,\tau} a_{t,\tau} = \xi_t \sum_{\tau=\tau_{Lt}}^{\tau_U} \phi_{t,\tau} a_{t,\tau} = \frac{R_t}{R'_t} R'_t = R_t \tag{25}$$

Because $R_t < R'_t$, $\xi_t < 1$ in this case. Therefore, Ineq. (20) establishes as far as $0 \le \phi_{t,\tau} \le 1$, which is assured by defining $\phi_{t,\tau}$ with the logistic function as Eq. (22). In Fig. 2, adjusted regeneration rate for a given regeneration intensity (black line) is shown as the dashed and dotted line. For the case of $R_t > R'_t$, the same preparation can violate Ineq. (20). To adhere to Ineq. (20), we adjusted the distance between $\phi_{t,\tau}$ and 1 (the upper horizontal line of Fig. 2), as we adjusted the distance between $\phi_{t,\tau}$ and 0 for the case of $R_t < R'_t$. $\psi_{t,\tau}$ and $\xi_t$ for $R_t > R'_t$ in Eqs. (23) and (24) represent this adjustment. In fact, the annual regeneration area of each stand age can be prepared so that Eq. (8) is satisfied as follows:

$$\begin{aligned} \sum_{\tau=\tau_{Lt}}^{\tau_U} r_{t,\tau} &= \sum_{\tau=\tau_{Lt}}^{\tau_U} [(1 - \xi_t) + \xi_t \phi_{t,\tau}] a_{t,\tau} = (1 - \xi_t) \sum_{\tau=\tau_{Lt}}^{\tau_U} a_{t,\tau} + \xi_t R'_t \\ &= \frac{(R'_t - R_t) \sum_{\tau=\tau_{Lt}}^{\tau_U} a_{t,\tau} + \left(R_t - \sum_{\tau=\tau_{Lt}}^{\tau_U} a_{t,\tau}\right) R'_t}{R'_t - \sum_{\tau=\tau_{Lt}}^{\tau_U} a_{t,\tau}} = R_t \end{aligned} \tag{26}$$

Thus, $\psi_{t,\tau}$ which assures Eqs. (8) and Ineq. (20) is prepared using a function whose range is [0, 1] for $\phi_{t,\tau}$ even for this case.

$r_{t,\tau}$ is now completely controlled by $k_R$, $g_R$, $\alpha_{\phi k}$, $\beta_{\phi k}$, $\alpha_{\phi g}$, and $\beta_{\phi g}$. That is, using the continuous approximation technique, we formulated the FHR model as the function of these six variables. If we simply combined the nonlinear models with ordinary formulation for the LP technique, and we established an FHR with $t_F = 100$ and $\tau_U = 250$, we had to optimize $r_{t,\tau}$ which totaled 25,000 (100 × 250). Even reducing the number of age-classes by defining age-class-1 with 1–5-year stands, and older as well, and reducing the number of time periods to every five years, we still had 1000 variables. Compared with this, our model has a substantially more compact search space. It is also notable that the number of decision variables in our model is independent of the gathering of the plural ages stands and length of the term. Even if $t_F = 150$, the dimension of the search space of our approach is 6, while that of ordinary formulation increases to 37,500. Hoganson and McDill [46] indicated that the time horizon of a FHR can be of interest. The independency of the dimension of $t_F$ indicates that we can also make $t_F$ as a decision variable. Therefore, we treated $t_F$ as a decision variable and optimized the seven variables simultaneously.

### 2.4. Achieving a normal forest

Although the assurance to achieve a given DNF (Eq. (10)) is easily implemented in the LP framework, our approach needs alternative efficient constraint for its assurance. We used the following constraint set which is stricter than Eq. (10):

$$R_t = R_{NF} \quad \forall\, t \in \{t_{NF} - \tau_{NF} + 1, \ldots, t_{NF}\} \tag{27}$$

$$t' = t - (t_F - \tau_{NF}) \tag{28}$$

$$\tau_{Lt} = \max\{\tau'_L,\ t'\} \tag{29}$$

$$\sum_{\tau=1}^{\tau'_L - t'} a'_{1,\tau} \le (\tau_{NF} - t')R_{NF} \quad \forall\ t' \in \{1, \ldots, \tau'_L - 1\} \tag{30}$$

where $t'$ denotes the time from $t_F - \tau_{NF}$ (year), $\tau'_L$ is a constant lower bound of regenerable stand age that should be given by planners considering the capacity of forest land use (year, $1 \le \tau'_L \le \tau_{NF}$), and $a'_{t',\tau}$ means $a_{t,\tau}$ with the relationship of Eq. (28), e.g., $a'_{1,\tau} = a_{t_F - \tau_{NF}+1,\tau}$. Eq. (27) regulates the control of annual total regeneration area for $\tau_{NF}$ years at the end of the schedule. Eqs. (28)–(29) are the minimum harvest age constraints that control the lower bound of regenerable age [47,48]. Ineq. (30) is the condition of age-class distribution to achieve the DNF with the controls.

The simplest control to achieve the DNF is to annually regenerate $R_{NF}$ ha stands for $\tau_{NF}$ years. Eq. (27) indicates ensuring such control during $\tau_{NF}$ years at the end of the schedule. In this regeneration, we also need to restrict the number of regenerations in a stand only once after starting the control. This restriction can be implemented by setting the lower bound of regenerable stand age ($\tau_{Lt}$) to be $t'$ of Eq. (28). However, we need to prevent clearcutting of stands younger than $\tau'_L$ to conserve the capacity of the forest. As a result, Eq. (29) should be used. Eq. (29) indicates that $\tau_{Lt} = \tau'_L$ while $t \le t_F - \tau_{NF}$.

For the control to succeed we must be able to ensure annual regeneration stands for $\tau_{NF}$ years continuously. This constraint is formulated as follows:

$$R_{NF} \le \sum_{\tau=\tau_{Lt}}^{\tau_U} a'_{t',\tau} \quad \forall\, t' \in \{1,\ 2, \ldots, \tau_{NF}\} \tag{31}$$

Although Ineq. (31) is simpler than Ineq. (30), it requires us to refer to the age-class distribution of $\tau_{NF}$ years to examine whether it establishes. On the other hand, Ineq. (30) only refers to the age-class distribution at $t' = 1$. Below it is explained that combining with Ineq. (31) and Eqs. (28) and (29), we obtain Ineq. (30). Let us use the following inequality, which is identical to Ineq. (30) because of Eq. (11), for this explanation instead:

$$t'R_{NF} \le \sum_{\tau=\tau'_L-(t'-1)}^{\tau_U} a'_{1,\tau} \quad \forall\ t' \in \{1,\ 2, \ldots, \tau'_L - 1\} \tag{32}$$

First, let us consider the case of $\tau_{Lt} = \tau'_L$ (i.e., $t' < \tau'_L$). When $t' = 1$, Ineq. (32) is simply equivalent to Ineq. (31). Let us assume that Ineq. (32) is valid for $t' = 1$ and that we could regenerate $R_{NF}$ stands. When $t' = 2$, stands whose ages were $\tau'_L - 1$ at $t' = 1$ grow to be $\tau'_L$-year-old, i.e., reach regenerable age. Hence, the total area that can be regenerated at $t' = 2$ is $\sum_{\tau=\tau'_L-1}^{\tau_U} a'_{1,\tau} - R_{NF}$. Similarly, the total area that can be regenerated at $t'$ is $\sum_{\tau=\tau'_L-(t'-1)}^{\tau_U} a'_{1,\tau} - (t'-1)R_{NF}$ provided that we could ensure regenerable stands at $t' - 1$ during the case. Therefore, whether we can ensure regenerable stand area continuously can be evaluated using Ineq. (32) for this case.

Next, let us consider the case of $\tau_{Lt} = t'$ (i.e., $t' \ge \tau'_L$) if Ineq. (32) has established. At the first year (i.e., $\tau_{Lt} = \tau'_L = t'$), all $a'_{t',\tau}$ such that $\tau < t'$ have become $R_{NF}$. Consequently, the total regenerable stand area has become $\tau_{NF}R_{NF} - (t'-1)\,R_{NF} = R_{NF} + (\tau_{NF} - t')R_{NF}$. This value is $\ge R_{NF}$ while $t' \le \tau_{NF}$. This means that if we could satisfy Ineq. (32), the area of regenerable stands after $t'$ becomes $\tau_{Lt}$ is naturally ensured. In conclusion, Ineq. (30) is the equivalent condition to Ineq. (31) if we use Eqs. (27)–(29).

In our framework, only Ineq. (30) can be violated when calculating the NPV with a given set of the seven variables. Additionally, because $\tau'_L \le \tau_{NF}$, the following inequality is stricter than Ineq. (30):

$$\frac{1}{\tau'_L - t'} \sum_{\tau=1}^{\tau'_L - t'} a'_{1,\tau} \le R_{NF} \quad \forall\ t' \in \{1,\ 2, \ldots, \tau'_L - 1\} \tag{33}$$

This inequality indicates that the mean stand area per stand age from $\tau = 1$ to a given stand age less than $\tau'_L$ should be equal to or less than $R_{NF}$. The inequality is satisfied if we control $R_t \le R_{NF}$ for $\tau'_L$ years each time. In our case, Eq. (18) manages $R_t$ in this way. Therefore, our model always produces feasible solutions.

## 3. Application

### 3.1. Subject region

We established FHRs for cedar (*Cryptomeria japonica* D. Don; "Ura" type), cypress (*Chamaecyparis obtusa* Sieb. & Zucc.), red pine (*Pinus densiflora* Sieb. & Zucc.), and larch (*Larix kaempferi* (Lamb.) Carr.) in Nagano Prefecture, Japan. Related parameters for these species are shown in Table 1.

The profitability of forestry in Japan is so low that clearcutting income is often less than planting cost, even without considering the discount rate with rotation age [49]. This is largely due to the high costs

**Table 1**
Parameters for each species.

| Parameter | Unit | Description | Cedar | Cypress | Red pine | Larch |
|---|---|---|---|---|---|---|
| $c_C$ †a | yen/m$^3$ | Clearcutting cost | 7716 | 8919 | 8419 | 5987 |
| $c_R$ †b | yen/ha | Reforestation cost | 2644,926 | 2651,926 | 1896,028 | 1788,228 |
| $\tau_{NF}$ †c | year | Rotation age of DNF | 58 | 60 | 55 | 52 |
| $\tau'_L$ †d | year | Lower bound of regenerable stand age | 40 | 45 | 40 | 40 |
| $R_{NF}$ †c | ha/year | Annual regeneration area of DNF | 225 | 157 | 123 | 2077 |
| $R_0$ †e | ha/year | Initial annual regeneration area | 1.282 | 9.478 | 0.037 | 5.340 |
| $Y'_{NF}$ †c | m$^3$/year | Annual yield of DNF | 154,559 | 80,635 | 48,084 | 767,785 |
| $Y'_0$ †f | m$^3$/year | Initial annual yield of clearcutting | 920 | 4999 | 10 | 2146 |
| $y_\infty$ †g | m$^3$/ha | Asymptote of mean yield of forests | 847.3 | 674.9 | 479.7 | 440.2 |
| $L_y$ †g | – | Location parameter of mean yield growth model | 1.066 | 1.050 | 1.116 | 1.114 |
| $k_y$ †g | 1/year | Steepness parameter of mean yield growth model | 0.0348 | 0.0258 | 0.0357 | 0.0416 |
| $m_y$ †g | – | Shape parameter of mean yield growth model | 1.37386 | 1.08077 | 1.20119 | 1.27443 |
| $p_S$ †b | yen/m$^3$ | Standard log price | 9795 | 12,269 | 9265 | 9088 |
| $p_L$ †h | yen/m$^3$ | Lower bound of log price | 5861 | 6282 | 7140 | 7140 |
| $p_U$ †h | yen/m$^3$ | Upper bound of log price | 13,800 | 17,376 | 12,780 | 12,780 |
| $k_p$ †h | – | Slope of log price model | –3525 | –20,251 | –8980 | –8980 |
| $U_{NF}$ †c | yen | Annual gain of DNF | $-3.321\cdot10^8$ | $-1.462\cdot10^8$ | $-1.925\cdot10^8$ | $-1.197\cdot10^9$ |

†a: Average clearcutting cost [87]. †b: Estimated cost in this region [76]. †c: The optimal rotation age of the normal forests [56], but modified for integer rotation ages. †d: "Standard rotation age" for each species [88]. †e: Annual artificially regenerated forest area [57]. †f: Estimated from the annual regeneration area assuming that clearcutting is done at $\tau_{NF}$-year-old. †g: See Appendix A. †h: See Appendix B.

of planting, weeding, and harvesting in a climate that enables diverse plants to regenerate naturally, and on a complex topography with steep slopes [50,51]. Consequently, from a purely economic perspective, the rational decision may be to abandon forestry in Japan. However, from an environmental perspective, it may be necessary to continue forestry to supply woods, thereby reducing global deforestation and $CO_2$ emissions. Consequently, the government set a policy target to increase the self-sufficiency rate of woods to 50% [52]. Even though up to 70% of the costs for planting and silviculture are subsidized [53], regeneration is rarely conducted. Smoothing of the age-class distributions is therefore recognized as a major national issue for forest management [49,54,55].

Because of low profitability in the region, the NPV of our application will be negative. Hence, although we maximize the NPV of profit, the practical aim is to minimize the NPV of deficit that will be compensated with a subsidy. Additionally, the objective function (Eq. (1)) indicates that not only the schedule to achieve the DNF but the DNF itself can be optimized. However, the optimal DNF would be empty (no forest) because of the low profitability of the region.

For the four species in Nagano Prefecture, the stands to be subsidized in order to achieve the required self-sufficiency rate were determined assuming the choice of optimal rotation age in each stand, minimization of annual expense for the subsidization, and stable age-class distribution [56]. Optimal rotation age usually changes with the site quality (biological site productivity). However, when a policy for spending the minimum subsidy on each stand is accepted, a normal forest is the optimal age distribution even when variation in the site quality is accounted for [56]. Therefore, we used the optimal normal forests with constraint of annual yield [56] as the DNF for each species. The normal forests are consistent with the DNFs in our case. For more detail of the normal forests and statistics of the subject forests, see Moriguchi et al. [56].

We used real age-class distributions of each species in 2012 [57] as the initial age-class distribution. We set $d = 0.08$, $\tau_U = 250$, $k_{Y'} = 0.12$, $g_{Y'} = 40$, $t_{Y'L} = 0$ and $t_{Y'U} = 80$ for each species. Other fixed parameters in the model are shown in Table 1. We set the ranges of decision variables which construct the search space as shown in Table 2. Note that $t_F$ should be an integer because it denotes the number of years to be simulated. Although the optimization of $t_F$ makes our problem MINLP, the effect of $t_F$ on the objective function is almost smooth (Fig. 3) because the year to achieve the DNF is fundamentally a continuous real number. However, the function is not unimodal. A profile of the objective function of cedar is shown in Fig. 4. We could not expect to find the global optimum using simple downhill methods because of the multimodal nature.

### 3.2. Optimization method

We used the simulated annealing (SA) [58,59] to find the optimal solutions. The probability of finding the global optimum using SA is theoretically proven to converge to one as computation time increases, when using particular "cooling" functions, which control the

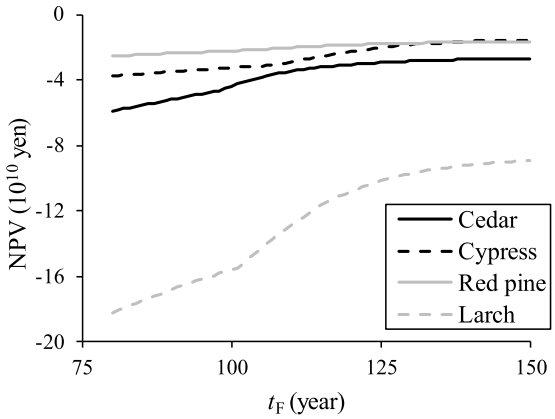


**Fig. 3.** Relationships between the values of the objective function and $t_F$. Values in the range of $80 \le t_F \le 150$ with $k_R = 0.1$, $\tau_R = 50$, $\alpha_{\phi g} = 120$, $\beta_{\phi g} = 120$, $\alpha_{\phi k} = 0.1$ and $\beta_{\phi k} = 0.1$.

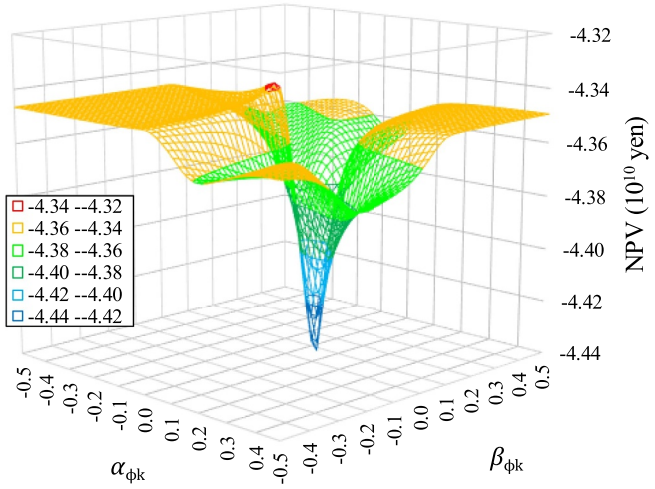


**Fig. 4.** Relationships between the values of the objective function and $\alpha_{\phi k}$ and $\beta_{\phi k}$. Values in the range of $-0.5 \le \alpha_{\phi k} \le 0.5$ and $-0.5 \le \beta_{\phi k} \le 0.5$ with $k_R = 0.1$, $\tau_R = 50$, $\alpha_{\phi g} = 120$, $\beta_{\phi g} = 120$ and $t_F = 100$.

"temperature" parameter, and corresponding proposal density functions, which suggest next candidate solutions [60–63]. The SA is a major method to optimize various scheduling problems [48,64,65].

In practice, the time that we can use for simulating the annealing process is limited. As a result, we usually use functions that experimentally elicit good performance [66,67]. We should also consider that the range of the objective function changes the efficiency of the optimization process. Appropriate parameters of the cooling function and the proposal density function should be explored for a given model.

Moriguchi et al. [68] explored the efficient implementation of

**Table 2**
The bounds of controllable variables to be optimized.

| Variable | Description | Lower bound | Upper bound | Interval in grid search †a |
|---|---|---|---|---|
| $k_R$ | Slope parameter of the scaled logistic function of the annual regeneration area | 0 | 0.5 | 0.05 |
| $g_R$ | Shift parameter of the scaled logistic function of the annual regeneration area | 0 | 150 | 15 |
| $\alpha_{\phi k}$ | Final value of the slope parameter of the logistic function of the regeneration intensity between stand ages | –0.5 | 0.5 | 0.1 |
| $\beta_{\phi k}$ | Initial value of the slope parameter of the logistic function of the regeneration intensity between stand ages | –0.5 | 0.5 | 0.1 |
| $\alpha_{\phi g}$ | Final value of the shift parameter of the logistic function of the regeneration intensity between stand ages | 0 | 150 | 15 |
| $\beta_{\phi g}$ | Initial value of the shift parameter of the logistic function of the regeneration intensity between stand ages | 0 | 150 | 15 |
| $t_F$ | The final year of the schedule (year) | 80 | 150 | 7 |

†a: The intervals in the grid search are set so that each variable has 11 candidates.

**Table 3**
Summary of results from grid searching and SA.

| Attributes | | Cedar | Cypress | Red pine | Larch |
|---|---|---|---|---|---|
| Grid search solutions | Maximum NPV (yen) †a | $-2.013\cdot10^{10}$ | $-8.157\cdot10^{9}$ | $-1.280\cdot10^{10}$ | $-5.328\cdot10^{10}$ |
| | Number of SA processes that provided higher NPVs †b | 1574 (25.2%) | 3368 (53.9%) | 4521 (72.3%) | 5569 (89.1%) |
| Parameters of reversed Weibull distribution †c | Shape | 0.227 | 0.190 | 0.170 | 0.223 |
| | Scale | $2.28\cdot10^{5}$ | $5.44\cdot10^{6}$ | $4.58\cdot10^{4}$ | $1.67\cdot10^{7}$ |
| | Location | $-2.013\cdot10^{10}$ | $-8.046\cdot10^{9}$ | $-1.273\cdot10^{10}$ | $-5.097\cdot10^{10}$ |
| | D statistic †d | 2.09 *** | 1.55 * | 1.65 ** | 2.12 *** |
| Parameters of reversed generalized Pareto distribution †c | Shape | 5.651 | 4.991 | 4.756 | 3.740 |
| | Scale | 421.9 | $2.35\cdot10^{4}$ | 205 | $3.49\cdot10^{5}$ |
| | Location | $-2.013\cdot10^{10}$ | $-8.046\cdot10^{9}$ | $-1.273\cdot10^{10}$ | $-5.097\cdot10^{10}$ |
| | D statistic †d | 1.24· | 1.01 | 1.14 | 1.99 ** |
| Best SA solution †e | Maximum NPV (yen) †a | $-2.013\cdot10^{10}$ | $-8.046\cdot10^{9}$ | $-1.273\cdot10^{10}$ | $-5.097\cdot10^{10}$ |
| | $k_R$ | 0.0482 | 0.0425 | 0.0380 | 0.0258 |
| | $g_R$ | 150.0 | 81.3 | 150.0 | 150.0 |
| | $\alpha_{\phi k}$ | 0.500 | 0.462 | 0.500 | 0.500 |
| | $\beta_{\phi k}$ | –0.424 | –0.500 | –0.415 | –0.388 |
| | $\alpha_{\phi g}$ | 82.0 | 116.8 | 83.8 | 112.1 |
| | $\beta_{\phi g}$ | 56.8 | 0.0 | 31.0 | 0.0 |
| | $t_F$ | 150 | 150 | 150 | 150 |

†a: Maximum NPVs are negative in these cases due to low profitability in the region. See Section 3.1. †b: Out of a total of 6250 processes. †c: Estimated using the maximum likelihood method with 50 NPVs produced by SA processes that used the same parameter with the best SA solution. †d: The D statistic of the Kolmogorov–Smirnov test. ·: 10%; *: 5%; **: 1%; ***: 0.1%. †e: The variables are detailed in Table 2.

simulated annealing for a thinning scheduling problem of a forest stand. They recommended the use of the geometric cooling function and the Cauchy distribution for the proposal density. Because the control performed well even in our case, we used the control with a modification in the definition of the energy function.

The acceptance probability of a proposed solution is as follows:

$$q = \min\left\{1, \exp\left(-\frac{E_{proposed} - E_{current}}{T}\right)\right\} \tag{34}$$

where $q$ is the acceptance probability, $E_{proposed}$ is the energy of a proposed solution, $E_{current}$ is the energy of the current state, and $T$ is the temperature parameter. The energy is minimized by the annealing process. Although the energy function can be simply defined with negative NPV (since NPV should be maximized), it should be noted that the temperature parameter depends on the scale of the objective function. Therefore, the energy function is scaled with the range of minimum and maximum values of the objective function obtained since the start of the annealing process [68]. The scale always keeps the value of the energy function in [0, 1] with the dynamic scaling parameter. By contrast, the energy function defined below provided better performance than the use of the dynamic method for the FHR problem:

$$E = \frac{-\mathrm{NPV}}{\mathrm{NPV}_{75} - \mathrm{NPV}_{25}} \tag{35}$$

where NPV indicates the objective function of Eq. (1), and $\mathrm{NPV}_{25}$ and $\mathrm{NPV}_{75}$ are 25% and 75% percentile NPVs obtained with 1000 evaluations of the objective function with complete random generation of solutions before the annealing process, respectively.

Similarly to Moriguchi et al. [68], we tested 125 parameter sets that were defined using five initial candidate temperatures of $10^{-0.6}$, $100^{\cdot0}$, …, $10^{1.8}$, five candidate rates of final temperature with initial temperatures in $10^{-1.0}$, $10^{-2.4}$, …, $10^{-6.6}$, and five candidate rates of the scaling parameter of the Cauchy distribution on the range of each decision variable in $10^{-0.0}$, $10^{-0.6}$, …, $10^{-2.4}$. The Cauchy distribution is the truncated version at the bounds of the decision variables. The median before the truncation is at the current value of the decision variable. We set the maximum iteration to be 500,000 and the number of temperature levels to be 500. We terminated the searching process if the maximum NPV was not updated for 50,000 consecutive iterations. We executed the SA process 50 times for each SA parameter set. As a result, we executed 6250 SA processes (125 parameter sets, 50 times) for each species. The solution that provided the maximum NPV is presented as the result of the SA process. The solution reported in this paper is the best solution (which provides maximum NPV) of all 6250 SA runs.

Because SA is a stochastic heuristic optimization technique, and its efficiency depends on subjective problems, whether the sufficient optimal solution could be found should often be evaluated. Bettinger et al. [69] discussed that comparison with solutions produced with techniques that can find the global optimum is ideal (Level 6 of [69]), and even if this procedure cannot be used, estimation of the global optimum using extreme value theory is a possible method for evaluation (Level 4 of [69]).

We used two approaches for evaluating optimality. One approach was a comparison with the optimum solutions provided by the grid search that evaluates the objective functions on lattice points in the search space. The range of each of the seven decision variables was divided evenly between eleven candidates (Table 2). We then generated a total of $11^7$ ($\approx 1.95 \cdot 10^7$) combinations, and we identified the solution that provided the highest NPV. This process provides an exact assessment of whether SA satisfied minimum quality in terms of imitating full enumeration. However, the coarseness of the grid in the search space limits the resolution of this evaluation. Therefore, we also utilized a statistical estimation of the NPV of the global optimal solution. This was done by collecting resultant NPVs of SA processes that ran with the best parameter set of SA (with which the maximum NPV was produced). A reversed three-parameter Weibull distribution is often used for this evaluation [69]; however, the distribution can be statistically rejected in some cases [65,70]. Thus, we also used a reversed generalized Pareto distribution, a type of extreme value distribution with finite support [71]. Each distribution was fitted with the maximum likelihood estimation (MLE). Using the Kolmogorov–Smirnov test, the goodness of fit was also evaluated. We validated the optimality using the estimated location parameters of the distributions.

### 3.3. Application results

#### 3.3.1. Optimality

The summary of optimization results is shown in Table 3. For each species, at least 25% of the SA processes provided NPVs higher than that of the grid search. For all species, the Kolmogorov–Smirnov test rejected the assumption that the NPVs produced by SA followed a

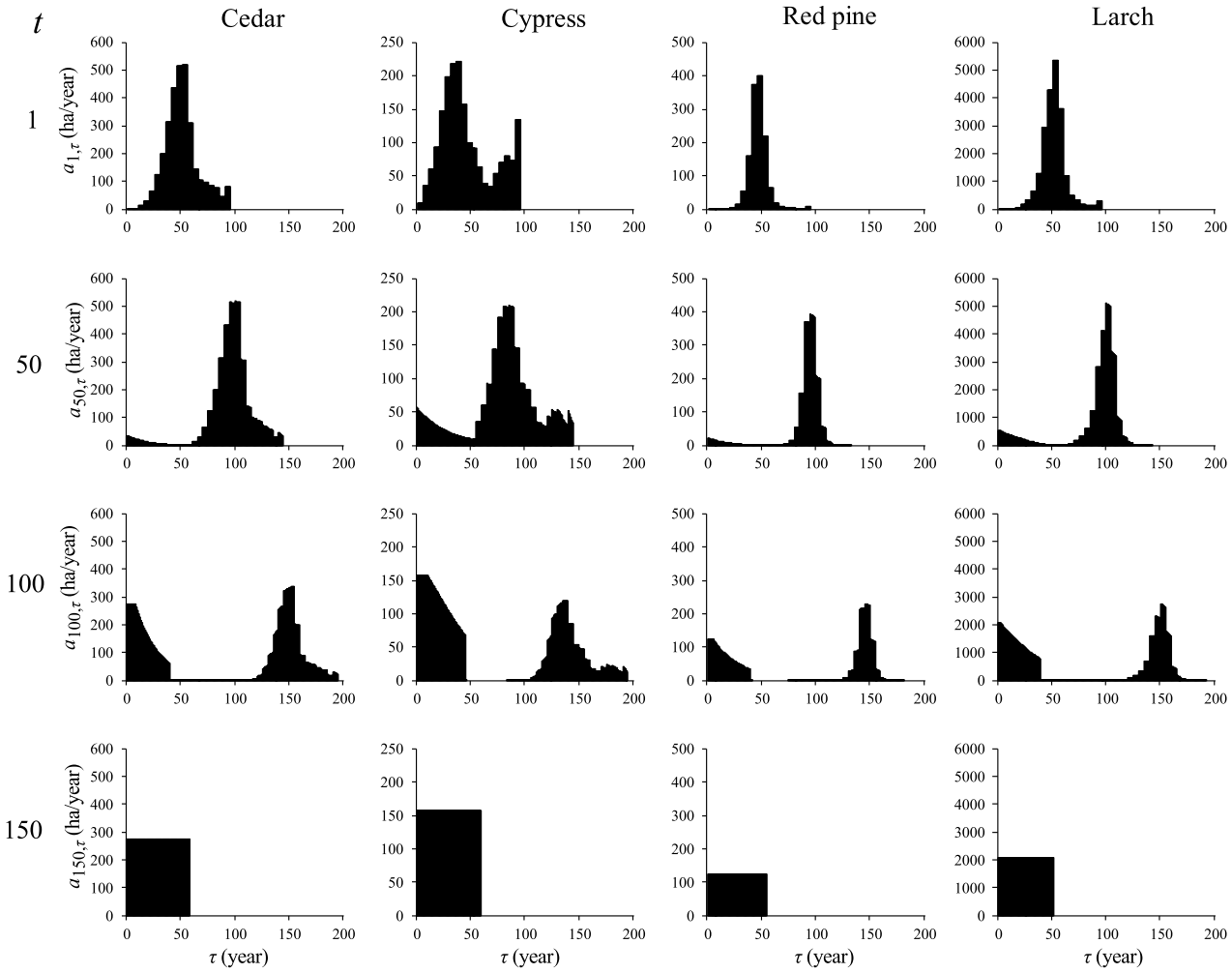


**Fig. 5.** Change-with-time of age-class distribution of each species.

reversed Weibull distribution with a 5% significance level. By contrast, the Kolmogorov–Smirnov test did not reject the assumption that the distribution of the NPVs followed a reversed generalized Pareto distribution, with the exception of larch, with a 5% significance level. For all estimations, the estimated location parameters were rarely different from the maximum NPVs. These results may indicate that the maximum NPVs that we obtained are sufficiently close to the global optima.

### 3.3.2. *Analysis of solutions*

Comparing the decision variables, it is clear that several decision variables are similar among species (Table 3). For example, $t_F$ is 150 for all species. This means the achievement of the DNF for these species should be delayed for as long as possible. Relatively small $k_R$ values indicate that the annual total regeneration area should be increased gradually. Suggestion to set $g_R$ equal to $t_F$, i.e., upper bound values, indicates the increase of annual total regeneration area should not be sigmoidal since there is no inflection point in $t < t_F$. The set of positive $\alpha_{\phi k}$ and negative $\beta_{\phi k}$ means the regeneration intensity should be high in old stands at the beginning of the schedule, then high in young stands later in the schedule. The values of $\alpha_{\phi g}$ and $\beta_{\phi g}$, which imply the inflection points of the regeneration intensity, have the relationship of $\alpha_{\phi g} > \beta_{\phi g}$; however, there are several variations compared with other decision variables. Age-class distributions simulated using the values in Table 3 are shown in Fig. 5. Compared with the plots at $t = 1$ and $t = 50$ of each species, we can confirm that regeneration is majorly done in old stands at the beginning of the schedule. By contrast, the plots at $t = 100$ show a complete division in age-class distribution caused by high regeneration intensity in young stands. Even with the division, each species finally achieved the DNF.

The annual total regeneration area, supply, log price, and income of FHR of each species simulated with the solutions in Table 3 are shown in Fig. 6. Controlling the annual total regeneration area so that it increases gradually, the solutions ensure a certain level of yield but maintains a low yield so that the log price remains high, especially at the beginning of the schedule. As a result, annual revenues for each species were positive at the beginning of the schedule. Since the NPV weights the revenues during the early period with a high present value factor, it is a logical strategy for maximizing the NPV. After a peak of the annual yield, it decreases with time and consequently, the log price increases. This is because the steepness parameter of regeneration intensity shifts from positive to negative, thereby the regeneration intensity shifts from the older stands to the younger stands. This control contributed to decreasing annual yields even with a constant annual total regeneration area in the final phase of the schedule. Although there was an increase in annual yield and a consequent decrease in log price at the end of the schedule, the present value factor is the lowest at the end of the schedule. Therefore, the reduction in NPV is minimized.

The Forestry Division of Nagano Prefectural Government [54] presented an FHR for the region for the next 80 years assuming a constant annual total regeneration area beginning immediately. Ordinary FHR often endeavors to achieve the DNF as quickly as possible, maybe based on the turnpike theory [72]. However, our results suggest a gradual increase in the annual total regeneration area. The log price models that take the balance of supply and demand into account worked as a

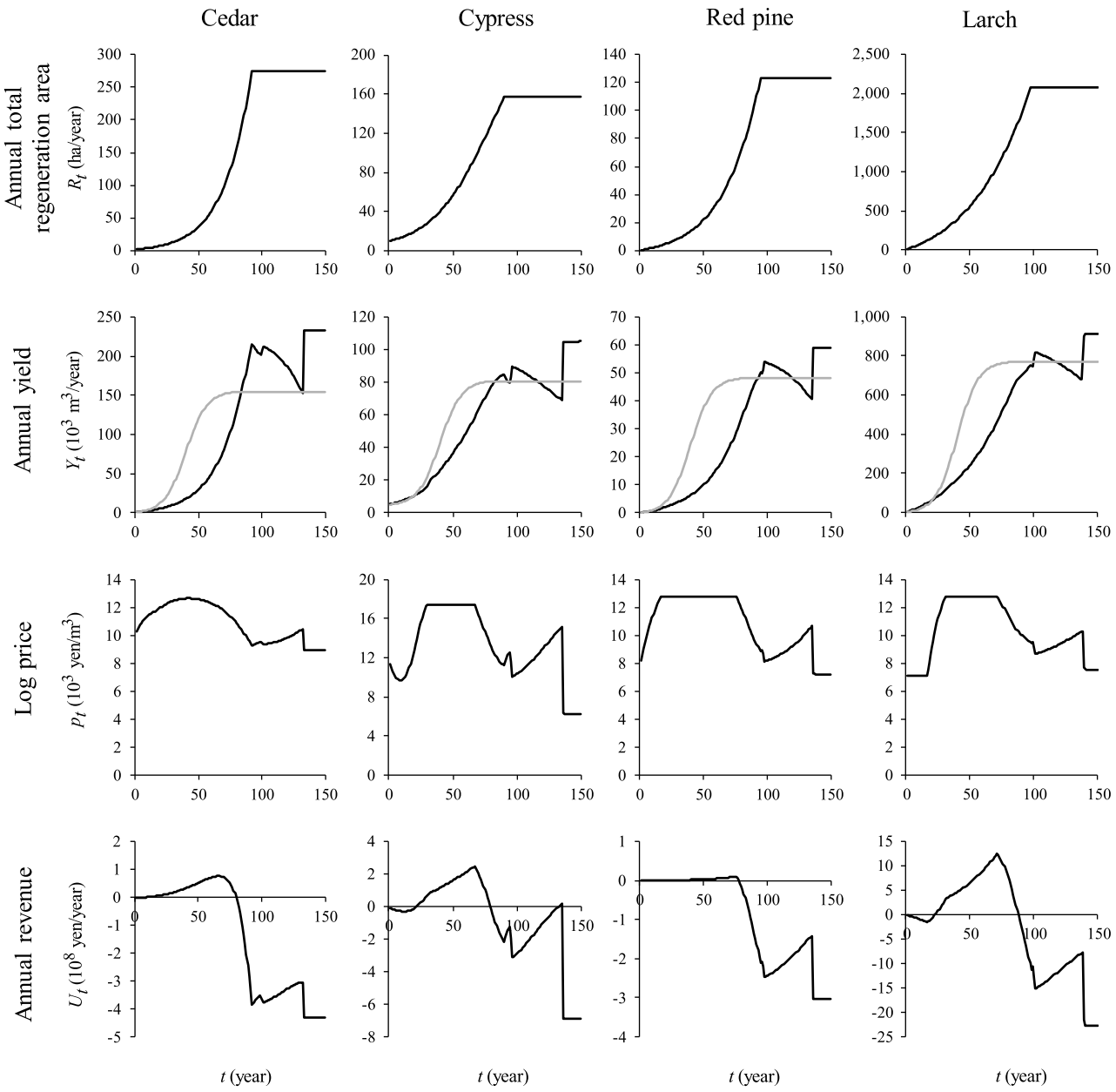


**Fig. 6.** Annual total regeneration area, annual yield, log price, and revenues. The solid grey lines in the plots of the annual yield indicate the supply that results in the log price equal to $p_S$.

natural "penalty function" in response to an overproduction. The suggestion of the delay in the achievement of the DNF seems reasonable since we used a DNF which is optimal involving a constraint on annual total yield [56]. In other words, the DNF is not purely optimal such that the turnpike theory assumes. Because the DNF requires a subsidy for supplying yield, the delay of the achievement is reasonable for maximizing the NPV.

While it is debatable whether we should allow higher regeneration intensity in younger stands, which results in a complete division of age-class distribution as shown at $t = 100$ (Fig. 5), it may be acceptable since it helps to increase NPV. However, preventing such age-class distribution can also be a possible management principle. For this case, it is possible to provide alternative solutions by constraining $\alpha_{\phi k}$ and $\beta_{\phi k}$ to positive values. The optimal solutions for this case are shown in Supplementary File 1. Modeling the regeneration intensity with other functions is also possible. Although we used the logistic function for the regeneration intensity, this requirement for the design is solely to make the values always in [0, 1]. Similarly, the requirement for the function of the annual total regeneration area is only Eq. (30). Therefore, any functions and controls which satisfy the requirements can be used instead of our application. The controls may even be procedures relating the adaptive forest management [73,74]. Although incorporating such complex controls with FHRs has been difficult, the reformulation with the continuous approximation technique may enable it.

## 4. Conclusions

In this paper, we presented a new modeling approach for establishing FHR with the continuous approximation technique [37]. The FHR problem was formulated as an optimization problem of a small number of parameters relating to the control of the dynamic of the age-class distribution. An efficient constraint to reduce solutions that cannot achieve a DNF at the end of the schedule was also developed. Our FHR model in Nagano Prefecture had seven parameters to be optimized. The

optimal solutions were obtained using SA. The solutions suggested a gradual increase in the annual total regeneration area and the delay of the achievement of the DNF, reflecting the low profitability of forestry of the region. The approach presented here allows the use of various nonlinear, or more complex, functions and models. Therefore, the developed approach may help us to explore effective forest management policies from various candidates.

In this study, we formulated the FHR problem assuming that a normal forest should be achievable at the end of the schedule. In our example case, the objective function was defined to minimize subsidies. Under this policy, normal forest was the optimal state in stable age-class distributions even with variation in the site quality [56]. On the other hand, an age-class distribution with variable rotation age of stands can also be stable [40], and in general cases, optimal rotation age can vary with the site quality [75]. Other factors such as planting and harvesting costs can also change optimal rotation age, even within a species. For such general cases, the age-class distribution with variable rotation age can be the optimal destination state of a species. Even for these cases, however, it is possible to establish FHR using our approach, by compiling forest stands separately with respect to stand conditions, in the same way we have compiled separate forest stands based on species in this study.

## CRediT authorship contribution statement

**Kai Moriguchi:** Conceptualization, Methodology, Software, Formal analysis, Writing - original draft. **Tatsuhito Ueki:** Supervision, Writing - review & editing. **Masashi Saito:** Supervision, Writing - review & editing.

## Declaration of Competing Interest

The authors declare that they have no known competing financial interests or personal relationships that could have appeared to influence the work reported in this paper.

## Acknowledgments

This work was supported by the Japan Society for the Promotion of Science KAKENHI [grant number 15H04508; 19K15872]. We thank Dai Otsuka for his fruitful suggestions during the early draft stages. We are also grateful for fruitful comments and suggestions from three anonymous reviewers and an associate editor of this journal.

## Supplementary materials

Supplementary material associated with this article can be found, in the online version, at doi:10.1016/j.orp.2020.100158.

## Appendices

### *Appendix A. Estimating parameters of yield growth model*

The yield model for a stand can be derived from the following equations [76]:

$$H_\tau = H_\infty[1 - L_H \exp(-k_H \tau)]^{m_H} \tag{A1}$$

$$w_\tau = \sigma H_\tau^\gamma \tag{A2}$$

$$y'_\tau = \omega w_\tau \tag{A3}$$

where $H_\tau$ is the mean height of the dominant trees at $\tau$-year-old (m), $w_\tau$ is the maximum capacity of stock of the stand at $\tau$-year-old ($m^3$/ha), $y'_\tau$ is the yield volume per area at $\tau$-year-old ($m^3$/ha), and $H_\infty$, $L_H$, $k_H$, $m_H$, $\sigma$, $\gamma$, and $\omega$ are given parameters. Eq. (A1) is modeled with the Bertalanffy–Richards model [44,45] that is usually used for modeling height growth [77,78]. Height growth models in this region assume that only $H_\infty$ in Eq. (A1) depends on the biological productivity of the site [56,79]. Eq. (A2) is a type of power-law that is commonly observed for full-density conditions [80,81]. $\omega$ is determined with the ratio parameters that represent the sparseness in standard managed forests and yield rate at clearcutting. Using Eqs. (A1) – (A3), the yield model for a stand is derived as follows:

$$y'_\tau = y'_\infty[1 - L_Y \exp(-k_Y \tau)]^{m_Y} \tag{A4}$$

where $y'_\infty = \sigma\omega H_\tau^\gamma$, $L_Y = L_H$, $k_Y = k_H$, and $m_Y = \gamma m_H$.

Moriguchi et al. [56] showed that the area frequency of $H_\infty$ in the region could be approximated with the generalized gamma distribution [82]. Because the distribution is closed with respect to allometric transformation [83], the distribution of $y'_\infty$ can also be approximated with generalized gamma distribution with parameter translation. Further, the set of forests stands to be managed for wood production in the region was determined as the stands whose $y'_\infty$ is in a limited range [56]. The model of mean yield of a set of forests is therefore formulated as follows:

$$\begin{aligned} y_\tau &= \int_{y'_{\infty L}}^{y'_{\infty U}} y'_\tau \frac{\mathrm{PDF}(y'_\infty; \cdot)}{\mathrm{CDF}(y'_{\infty U}; \cdot) - \mathrm{CDF}(y'_{\infty L}; \cdot)} dy'_\infty \\ &= y_\infty[1 - L_Y \exp(-k_Y a)]^{m_Y} \end{aligned} \tag{A5}$$

where

$$y_\infty = \frac{\int_{y'_{\infty L}}^{y'_{\infty U}} y'_\infty \mathrm{PDF}(y'_\infty; \cdot) dy'_\infty}{\mathrm{CDF}(y'_{\infty U}; \cdot) - \mathrm{CDF}(y'_{\infty L}; \cdot)}$$

where $y'_{\infty L}$ and $y'_{\infty U}$ are the lower and upper limits of $y'_\infty$ in the set of forests, respectively, and $\mathrm{PDF}(y'_\infty; \cdot)$ and $\mathrm{CDF}(y'_\infty; \cdot)$ represent the probability density function and cumulative density function of $y'_\infty$, respectively. $L_Y$, $k_Y$, $m_Y$, $y'_{\infty L}$ and $y'_{\infty U}$, and parameters of the distributions of $y'_\infty$ were estimated by [56].

*Appendix B. Log price model*

Because we planned an FHR of all forests for wood production in the region, we used a monopolistic price model, which assumes that the log price in the region is completely controlled by the annual total yield from the set of forests. With the monopolistic price model, the demand curve gives the price of a given supply. In practice, log price may have minimum and maximum bounds reflecting that imports to and exports from other regions work to prevent extreme log prices. Further, we assume that the log demand will basically increase in the future, considering consistency with the policy target [52]. Consequently, the annual total yield relative to the $Y'_t$ (annual total yield that realizes the "standard" price) is used as the argument of the demand curve (Fig. B.1). As a result, we modeled the log price model as Eq. (13).

We estimated the slope of the log price ($k_p$) based on the relationship between the annual log prices of middle-diameter 3.65–4.0 m length logs

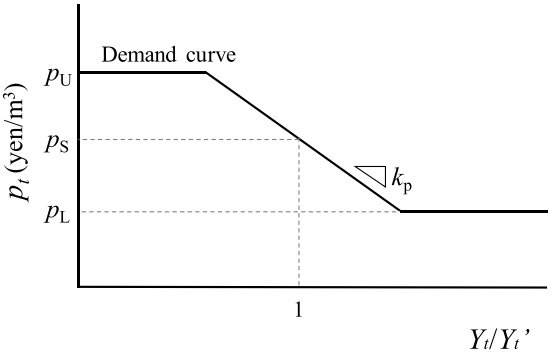


**Fig. B.1.** Assumed log price model. Because annual demand is assumed to change with time, the log price is formulated as the relationship with annual total yield ($Y_t$) relative to the yield that makes the log price be $p_S$ ($Y'_t$). The demand curve provides the price in the monopolistic price model. Upper and lower bounds are set to incorporate the prevention of extreme prices by imports to and exports from other regions.

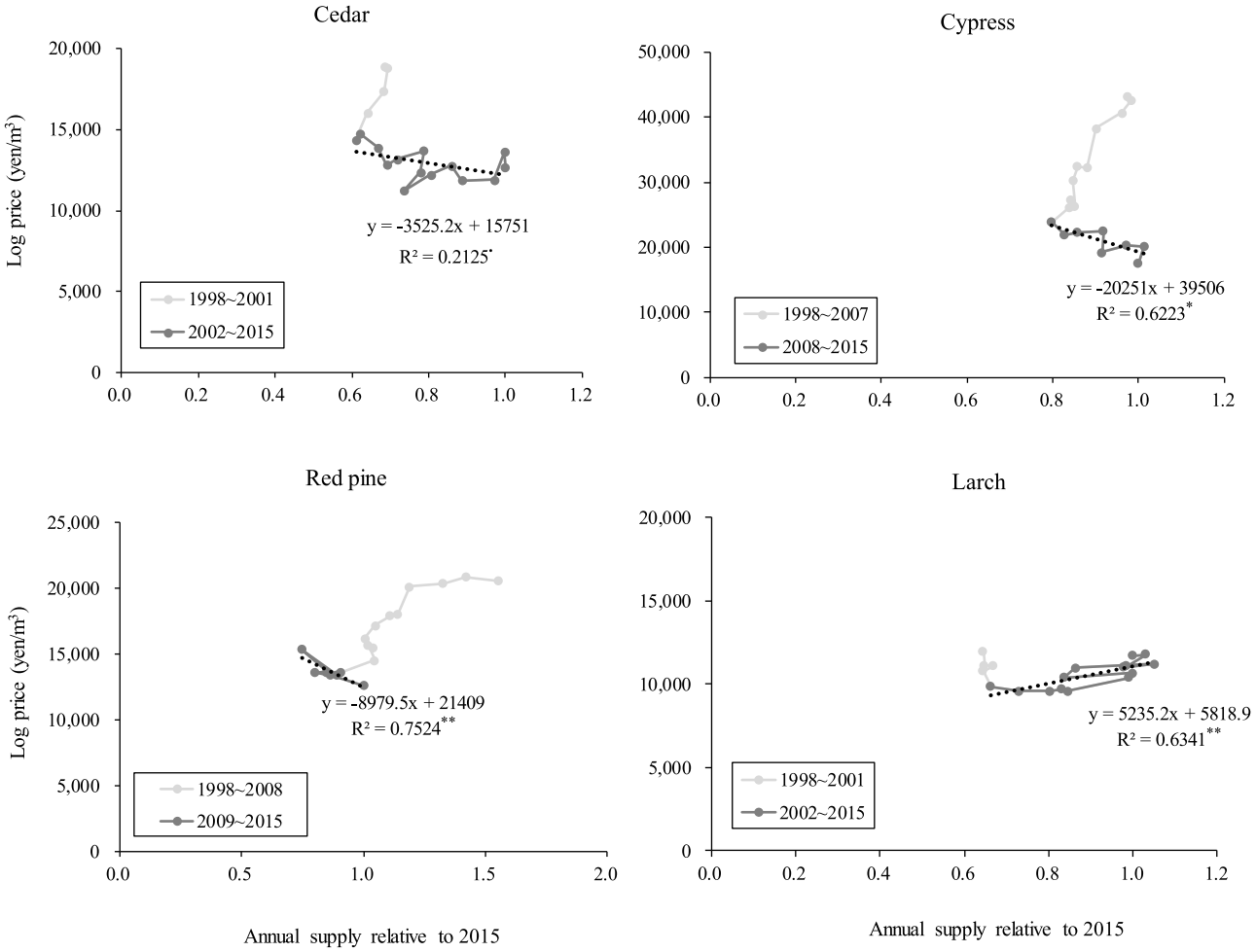


**Fig. B.2.** Relationship between log price and annual supply for each species from 1998 to 2015. Log price is the price of middle-diameter 3.65–4.0 m length logs [84]. The log price is standardized using the consumer price index of 2015 [89]. The annual supply of each species is standardized against the supply during 2015. Significance level: ·: 10%; *: 5%; **: 1%.

[84] and the annual supply of logs relative to that of 2015 [85] (Fig. B.2). To avoid the problem of identification [86], we should use only data in a term where the demand curve was stable for the estimation. For the estimation of slopes, we used only the data shown with black points in Fig. B.2. For larch, the actual demand structure has been changing in recent years and therefore, the relationship between the supply and log price in Fig. B.2 cannot be interpreted as a normal demand curve. Therefore, we used the parameters of red pine, whose wood characteristics are most similar to those of larch among the other species, for the larch model. The lower bound ($p_L$) and the upper bound ($p_U$) are determined with three times the range of the log prices of the fitting data.

## References


[1] Penttinen MJ. Impact of stochastic price and growth processes on optimal rotation age. Eur J For Res 2006;125:335–43https://doi.org/10.1007/s10342-006-0117-7.
[2] Vettenranta J, Miina J. Optimizing thinnings and rotation of Scots pine and Norway spruce mixtures. Silva Fenn 1999;33:73–84https://doi.org/10.14214/sf.671.
[3] Toyama K, Aruga K, Suzuki Y. Correlation of woody biomass demand with optimum rotation age and thinning regime in Northern Tochigi Prefecture, Japan. J Jpn Soc 2017;99:251–8https://doi.org/10.4005/jjfs.99.251.
[4] Miles L, Kapos V. Reducing greenhouse gas emissions from deforestation and forest degradation: global land-use implications. Science 2008;320:1454–5https://doi.org/10.1126/science.1155358.
[5] Betts MG, Wolf C, Ripple WJ, Phalan B, Millers KA, Duarte A, et al. Global forest loss disproportionately erodes biodiversity in intact landscapes. Nature 2017;547:441–4https://doi.org/10.1038/nature23285.
[6] Kaya A, Bettinger P, Boston K, Akbulut R, Ucar Z, Siry J, et al. Optimisation in forest management. Curr For Rep 2016;2:1–17https://doi.org/10.1007/s40725-016-0027-y.
[7] Borges P, Bergseng E, Eid T. Adjacency constraints in forestry: a simulated annealing approach comparing different candidate solution generators. Math Comput For Nat Sci 2014;6:11–25.
[8] Nakajima T, Kanomata H, Matsumoto M. Visualization of optimized solution space using a simulation system for the development of local forest management planning. Ann Forest Res 2016;59:117–28https://doi.org/10.15287/afr.2016.556.
[9] Bettinger P, Boston K, Kim Y-H, Zhu J. Landscape-level optimization using tabu search and stand density-related forest management prescriptions. Eur J Oper Res 2007;176:1265–82https://doi.org/10.1016/j.ejor.2005.09.025.
[10] Boston K, Sessions J, Rose R, Hoskins W. Incorporating regeneration effort as a decision variable in tactical harvest scheduling. West J Appl For 2009;24:61–6https://doi.org/10.1093/wjaf/24.2.61.
[11] Dong L, Bettinger P, Qin H, Liu Z. Reflections on the number of independent solutions for forest spatial harvest scheduling problems: a case of simulated annealing. Silva Fenn 2018;52:7803https://doi.org/10.14214/sf.7803.
[12] Kent B, Bare BB, Field RC, Bradley GA. Natural resource land management planning using large-scale linear programs: the USDA Forest Service experience with FORPLAN. Oper Res 1991;39:13–27.
[13] Başkent EZ, Keleş S. Developing alternative wood harvesting strategies with linear programming in preparing forest management plans. Turkish J Agric For 2006;30:67–79https://doi.org/10.3906/tar-0501-6.
[14] Kidd WE, Thompson EF, Hoepner PH. Forest regulation by linear programming: a case study. J For 1966;64:611–3https://doi.org/10.1093/jof/64.9.611.
[15] Lappi J, Lempinen R. A linear programming algorithm and software for forest-level planning problems including factories. Scand J For Res 2014;29:178–84https://doi.org/10.1080/02827581.2014.886714.
[16] Kojima M, Mizuno S, Yoshise A. A primal-dual interior point algorithm for linear programming. Progress in mathematical programming. New York: Springer; 1989. p. 29–47https://doi.org/10.1007/978-1-4613-9617-8_2.
[17] Chubanov S. A polynomial projection algorithm for linear feasibility problems. Math Program 2015;153:687–713https://doi.org/10.1007/s10107-014-0823-8.
[18] Karmarkar N. A new polynomial-time algorithm for linear programming. Combinatorica 1984;4:373–95https://doi.org/10.1007/BF02579150.
[19] Hahn WA, Härtl F, Irland LC, Kohler C, Moshammer R, Knoke T. Financially optimized management planning under risk aversion results in even-flow sustained timber yield. For Policy Econ 2014;42:30–41https://doi.org/10.1016/j.forpol.2014.02.002.
[20] Awasthi A, Omrani H. A goal-oriented approach based on fuzzy axiomatic design for sustainable mobility project selection. Int J Syst Sci Oper Logist 2019;6:86–98https://doi.org/10.1080/23302674.2018.1435834.
[21] Padberg M. Approximating separable nonlinear functions via mixed zero-one programs. Oper Res Lett 2000;27:1–5https://doi.org/10.1016/S0167-6377(00)00028-6.
[22] Gharaei A, Karimi M, Hoseini Shekarabi SA. An integrated multi-product, multi-buyer supply chain under penalty, green, and quality control polices and a vendor managed inventory with consignment stock agreement: the outer approximation with equality relaxation and augmented penalty algorithm. Appl Math Model 2019;69:223–54https://doi.org/10.1016/j.apm.2018.11.035.
[23] Giri BC, Bardhan S. Coordinating a supply chain with backup supplier through buyback contract under supply disruption and uncertain demand. Int J Syst Sci Oper Logist 2014;1:193–204https://doi.org/10.1080/23302674.2014.951714.
[24] Giri BC, Masanta M. Developing a closed-loop supply chain model with price and quality dependent demand and learning in production in a stochastic environment. Int J Syst Sci Oper Logist 2020;7:147–63. (in press). https://doi.org/10.1080/23302674.2018.1542042.
[25] Yin S, Nishi T, Zhang G. A game theoretic model for coordination of single manufacturer and multiple suppliers with quality variations under uncertain demands. Int J Syst Sci Oper Logist 2016;3:79–91https://doi.org/10.1080/23302674.2015.1050079.
[26] Heaps T. Convergence of optimal harvesting policies to a normal forest. J Econ Dyn Control 2015;54:74–85https://doi.org/10.1016/j.jedc.2015.03.001.
[27] Mitra T, Wan HY. Some theoretical results on the economics of forestry. Rev Econ Stud 1985;52:263–82https://doi.org/10.2307/2297621.
[28] Mitra T, Wan HY. On the faustmann solution to the forest management problem. J Econ Theory 1986;40:229–49https://doi.org/10.1016/0022-0531(86)90073-6.
[29] Salo S, Tahvonen O. On equilibrium cycles and normal forests in optimal harvesting of tree vintages. J Environ Econ Manag 2002;44:1–22https://doi.org/10.1006/jeem.2001.1224.
[30] Salo S, Tahvonen O. On the economics of forest vintages. J Econ Dyn Control 2003;27:1411–35https://doi.org/10.1016/S0165-1889(02)00065-9.
[31] Piazza A, Pagnoncelli BK. The stochastic Mitra–Wan forestry model: risk neutral and risk averse cases. J Econ 2015;115:175–94https://doi.org/10.1007/s00712-014-0414-4.
[32] Rautiainen O, Pukkala T, Miina J. Optimising the management of even-aged *Shorea robusta* stands in southern Nepal using individual tree growth models. For Ecol Manag 2000;126:417–29https://doi.org/10.1016/S0378-1127(99)00112-7.
[33] Kogler C, Rauch P. A discrete-event simulation model to test multimodal strategies for a greener and more resilient wood supply. Can J For Res 2019;49:1298–310https://doi.org/10.1139/cjfr-2018-0542.
[34] Shahi S, Pulkki R. A simulation-based optimization approach to integrated inventory management of a sawlog supply chain with demand uncertainty. Can J For Res 2015;45:1313–26https://doi.org/10.1139/cjfr-2014-0373.
[35] Lyon KS, Sedjo RA. An optimal control theory model to estimate the regional long-term supply of timber. For Sci 1983;29:798–812.
[36] Tsao Y-C. Design of a carbon-efficient supply-chain network under trade credits. Int J Syst Sci Oper Logist 2015;2:177–86https://doi.org/10.1080/23302674.2015.1024187.
[37] Newell GF. Dispatching policies for a transportation route. Transp Sci 1971;5:91–105.
[38] Newell GF. Scheduling, location, transportation, and continuum mechanics: some simple approximations to optimization problems. SIAM J Appl Math 1973;25:346–60https://doi.org/10.1137/0125037.
[39] Colombo SJ, Chen J, Ter-Mikaelian MT, McKechnie J, Elkie PC, MacLean HL, et al. Forest protection and forest harvest as strategies for ecological sustainability and climate change mitigation. For Ecol Manag 2012;281:140–51https://doi.org/10.1016/j.foreco.2012.06.016.
[40] Nagumo H, Koike A. Studies on the construction of management plans for private forests (I): determination of harvests and cutting areas of artificial forests for constructing a district forest plan. J Jpn For Soc 1981;63:79–89.
[41] Wan H. Revisiting the Mitra-Wan tree farm. Int Econ Rev 1994;35:193–8https://doi.org/10.2307/2527097.
[42] Baumol WJ, Benhabib J. Chaos: significance, mechanism, and economic applications. J Econ Perspect 1989;3:77–105https://doi.org/10.1257/jep.3.1.77.
[43] Bettinger P, Boston K, Siry JP, Grebner DL. Forest management and planning. Burlington MA: Academic Press; 2009.
[44] Bertalanffy L. Quantitative laws in metabolism and growth. Q Rev Biol 1957;32:217–31https://doi.org/10.1086/401873.
[45] Richards FJ. A flexible growth function for empirical use. J Exp Bot 1959;10:290–301https://doi.org/10.1093/jxb/10.2.290.
[46] Hoganson HM, McDill ME. More on forest regulation: an LP perspective. For Sci 1993;39:321–47.
[47] Liu WY, Lin CC. Spatial forest resource planning using a cultural algorithm with problem-specific information. Environ Model Softw 2015;71:126–37https://doi.org/10.1016/j.envsoft.2015.06.002.
[48] Bettinger P, Graetz D, Boston K, Sessions J, Chung W. Eight heuristic planning techniques applied to three increasingly difficult wildlife planning problems. Silva Fenn 2002;36:561–84https://doi.org/10.1007/978-94-017-0307-9_24.
[49] Japan Forestry Agency. Annual report on forest and forestry in Japan of fiscal 2016, http://www.rinya.maff.go.jp/j/kikaku/hakusyo/28hakusyo/index.html; 2017[accessed 28 December 2019].
[50] Fukumoto K, Ota T, Mizoue N, Yoshida S, Teraoka Y, Kajisa T. The effect of weeding frequency and timing on the height growth of young sugi (*Cryptomeria Japonica*) in southwestern Japan. J For Res 2017;22:204–7https://doi.org/10.1080/13416979.2017.1322347.
[51] Iwai Y. Forestry and the forest industry in japan. Vancouver: UBC Press; 2002.
[52] Japan Forestry Agency. The master plan of forest and forestry, http://www.rinya.maff.go.jp/j/kikaku/plan; 2016[accessed 28 December 2019].
[53] Japan Forestry Agency. Outline of subsidy system for forest management,http://www.rinya.maff.go.jp/j/seibi/zourinkikaku/shinrinseibi_aramashi.html; 2018[accessed 28 December 2019].
[54] Forestry Division of Nagano Prefectural Government. Guide for forest management

in Nagano Prefecture, http://www.pref.nagano.lg.jp/rinsei/sangyo/ringyo/shisaku/shishin/kaite.html; 2010[accessed 28 December 2019].
[55] Shiraishi N, Ookubo K, Hiroshima T. Study on a methodology for assessing maturity and sustainability of forest resources. J For Plan 2006;40:267–76.
[56] Moriguchi K, Ueki T, Saito M. Determining subsidised forest stands to satisfy required annual wood yield with minimum governmental expense. Land use policy 2017;67:573–83https://doi.org/10.1016/j.landusepol.2017.07.002.
[57] Japan Forestry Agency. Summary of forest resources at 31 March 2012, http://www.rinya.maff.go.jp/j/keikaku/genkyou/h24/index.html; 2013[accessed 28 December 2019].
[58] Černý V. Thermodynamical approach to the traveling salesman problem: an efficient simulation algorithm. J Optim Theory Appl 1985;45:41–51https://doi.org/10.1007/BF00940812.
[59] Kirkpatrick S, Gelatt CD, Vecchi MP. Optimization by simulated annealing. Science 1983;220:671–80https://doi.org/10.1126/science.220.4598.671.
[60] Szu H, Hartley R. Fast simulated annealing. Phys Lett A 1987;122:157–62https://doi.org/10.1016/0375-9601(87)90796-1.
[61] Ingber L. Very fast simulated re-annealing. Math Comput Model 1989;12:967–73https://doi.org/10.1016/0895-7177(89)90202-1.
[62] Geman S, Geman D. Stochastic relaxation, Gibbs distributions, and the Bayesian restoration of images. IEEE Trans Pattern Anal Mach Intell 1984;6:721–41https://doi.org/10.1109/TPAMI.1984.4767596.
[63] Tsallis C, Stariolo DA. Generalized simulated annealing. Phys A Stat Mech Its Appl 1996;233:395–406https://doi.org/10.1016/S0378-4371(96)00271-3.
[64] Duan C, Deng C, Gharaei A, Wu J, Wang B. Selective maintenance scheduling under stochastic maintenance quality with multiple maintenance actions. Int J Prod Res 2018;56:7160–78https://doi.org/10.1080/00207543.2018.1436789.
[65] Dong L, Bettinger P, Liu Z, Qin H. A comparison of a neighborhood search technique for forest spatial harvest scheduling problems: a case study of the simulated annealing algorithm. For Ecol Manag 2015;356:124–35https://doi.org/10.1016/j.foreco.2015.07.026.
[66] Ingber L. Simulated annealing: practice versus theory. Math Comput Model 1993;18:29–57https://doi.org/10.1016/0895-7177(93)90204-C.
[67] Connolly DT. An improved annealing scheme for the QAP. Eur J Oper Res 1990;46:93–100https://doi.org/10.1016/0377-2217(90)90301-Q.
[68] Moriguchi K, Ueki T, Saito M. Identification of effective implementations of simulated annealing for optimizing thinning schedules for single forest stands. Eur J Oper Res 2017;262:1094–108https://doi.org/10.1016/j.ejor.2017.04.037.
[69] Bettinger P, Sessions J, Boston K. A review of the status and use of validation procedures for heuristics used in forest planning. Math Comput For Nat Sci 2009;1:26–37.
[70] Boston K, Bettinger P. An analysis of Monte Carlo integer programming, simulated annealing, and tabu search heuristics for solving spatial harvest scheduling problems. For Sci 1999;45:292–301.
[71] van Montfort MAJ, Witter J V. The generalized Pareto distribution applied to rainfall depths. Hydrol Sci J 1986;31:151–62https://doi.org/10.1080/02626668609491037.
[72] McKenzie LW. Turnpike theory. Econometrica 1976;44:841–65https://doi.org/10.2307/1911532.
[73] Yamada Y, Yamaura Y. Decision support system for adaptive regional-scale forest management by multiple decision-makers. Forests 2017;8:453https://doi.org/10.3390/f8110453.
[74] Williams BK. Adaptive management of natural resources-framework and issues. J Environ Manag 2011;92:1346–53https://doi.org/10.1016/j.jenvman.2010.10.041.
[75] Marutani T. The effect of site quality on economically optimal stand management. J For Econ 2010;16:35–46https://doi.org/10.1016/j.jfe.2009.05.001.
[76] Moriguchi K, Ueki T, Otsuka D, Saito M. A simple method to calculate the upper limits on silviculture cost. J Jpn For Soc 2016;98:31–8https://doi.org/10.4005/jjfs.98.31.
[77] Tahvanainen T, Forss E. Individual tree models for the crown biomass distribution of Scots pine, Norway spruce and birch in Finland. For Ecol Manag 2008;255:455–67https://doi.org/10.1016/j.foreco.2007.09.035.
[78] Nishizono T, Kitahara F, Iehara T, Mitsuda Y. Geographical variation in age-height relationships for dominant trees in Japanese cedar (*Cryptomeria japonica* D. Don) forests in Japan. J For Res 2014;19:305–16https://doi.org/10.1007/s10310-013-0416-z.
[79] Katakura M, Yamanouchi M, Furukawa H. A study of long rotation management for artifictial stands of Japanese cypress and Japanese larch. Bull Nagano Prefect For Res Cent 2005;19:1–16.
[80] Burkhart HE. Comparison of maximum size–density relationships based on alternate stand attributes for predicting tree numbers and stand growth. For Ecol Manag 2013;289:404–8https://doi.org/10.1016/j.foreco.2012.10.041.
[81] Yoda K, Kira T, Ogawa H, Hozumi K. Self-thinning in overcrowded pure stands under cultivated and natural conditions. J Inst Polytech Osaka City Univ 1963;14:107–29.
[82] Stacy EW. A generalization of the gamma distribution. Ann Math Stat 1962;33:1187–92https://doi.org/10.2307/2237889.
[83] Khodabin M, Ahmadabadi A. Some properties of generalized gamma distribution. Math Sci 2010;4:9–28.
[84] Japanese Ministry of Agriculture, Forestry and Fisheries. Statistics of log price at 2017, http://www.maff.go.jp/j/tokei/kouhyou/mokuryu/kakaku/; 2017[accessed 28 December 2019].
[85] Japanese Ministry of Agriculture, Forestry and Fisheries. Demand and supply of wood production in Japan, http://www.maff.go.jp/j/tokei/kouhyou/mokuzai_zyukyu/; 2018[accessed 28 December 2019].
[86] Koopmans TC. Identification problems in economic model construction. Econometrica 1949;17:125–44https://doi.org/10.2307/1905689.
[87] Policy Planning Division of Japan Forestry Agency. Report of cost for log production at fiscal 2011. Policy Planning Division of Japan Forestry Agency; 2013.
[88] Forestry Division of Nagano Prefectural Government. 13th forest management plan in the lower region of the Chikuma river, http://www.pref.nagano.lg.jp/rinsei/sangyo/ringyo/shisaku/keikaku/h26tishinkei.html; 2014[accessed 28 December 2019].
[89] Japanese Ministry of Internal Affairs and Communications. Annual consumer price index (estimated expect for food and imputed service of owner-occupied dwellings), http://www.e-stat.go.jp/SG1/estat/List.do?bid=000001074279cycode=0; 2018[accessed 28 December 2019].